

Current Implicit Policies May Not Eradicate COVID-19

Ali Jadbabaie^{a,b}, Arnab Sarker^a, and Devavrat Shah^{a,c}

^aInstitute for Data, Systems, and Society, MIT

^bDepartment of Civil and Environmental Engineering, MIT

^cDepartment of Electrical Engineering and Computer Science, MIT

March 2022

Abstract

Successful predictive modeling of epidemics requires an understanding of the implicit feedback control strategies which are implemented by populations to modulate the spread of contagion. While this task of capturing endogenous behavior can be achieved through intricate modeling assumptions, we find that a population’s reaction to case counts can be described through a second order affine dynamical system with linear control which fits well to the data across different regions and times throughout the COVID-19 pandemic. The model fits the data well both in and out of sample across the 50 states of the United States, with comparable R^2 scores to state of the art ensemble predictions. In contrast to recent models of epidemics, rather than assuming that individuals directly control the contact rate which governs the spread of disease, we assume that individuals control the rate at which they vary their number of interactions, i.e. they control the derivative of the contact rate. We propose an implicit feedback law for this control input and verify that it correlates with policies taken throughout the pandemic. A key takeaway of the dynamical model is that the “stable” point of case counts is non-zero, i.e. COVID-19 will not be eradicated under the current collection of policies and strategies, and additional policies are needed to fully eradicate it quickly. Hence, we suggest alternative implicit policies which focus on making interventions (such as vaccinations and mobility restrictions) a function of cumulative case counts, for which our results suggest a better possibility of eradicating COVID-19.

1 Introduction

Determining the optimal policy for regulating an epidemic requires assessing complex infection dynamics across heterogenous populations. Due to this complexity, simplified models of epidemic spread are often used in order to develop guidelines and understand the impact of policies on the level of infection. Throughout the COVID-19 pandemic, a wide range of models have been implemented in order to both provide forecasts for important time series related to the pandemic as well as estimate causal effects of various policies [5, 15]. Such approaches have been developed since as early as the 19th century, and have been successfully applied to forecast epidemics such as seasonal influenza, smallpox, and H1N1 [9].

However, a key distinction between the COVID-19 pandemic and the spread of infectious disease in the past is the extent to which populations have reacted to limit the spread of the virus. As cases have surged, government officials have instituted lockdowns and mask mandates, individuals have changed their behavior at an unprecedented scale, and the public has received access to mass vaccination. This endogenous response to the state of the pandemic is rarely reflected by models developed for previous epidemics, but is critical in developing a robust response to COVID-19 [17, 18]. Even of the models used for COVID-19 death forecasting, only one explicitly includes an assumption that policy changes as the state of the pandemic worsens [14]. That is not to say that other models do not account for behavior. Rather, the remaining predictive models which do account for behavior treat human intervention as an exogenous variable, observed for example through mobility data and the presence of government mandates and vaccinations. In this work, we identify a model for epidemics where the response to the pandemic is encoded as an endogenous feature which depends on the magnitude of cases so far.

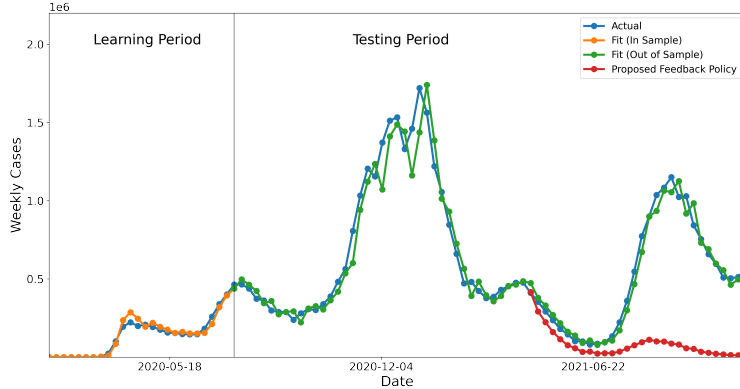


Figure 1: US Case counts as modeled by the dynamical system in Eq. (5). We learn the parameters of the control β_1 and β_2 on the first 30 weeks of data, and then they are held constant for the remainder of the data. One week ahead predictions using this method are shown in orange (in-sample) and green (out of sample), and the true data is shown in blue. For the in-sample time series, the model fits the data with an R^2 value of 0.966, and for the out of sample time series, the R^2 value is 0.949. In comparison, the 1 week ahead forecasts of state of the art ensemble predictions over the same period is 0.942 [15]. The red line represents a transition to a separate proposed policy which incorporates an integral feedback term, as discussed in [Rethinking Control for Future Epidemics](#).

1.1 Model Description

We begin by considering a general model of the growth phase of an epidemic with a time-varying growth rate, which we show contains several common epidemic models as special cases. We let $I(t)$ represent the number of infections in a population at time t , where t is a discrete time index, and use the convention $I(0) = 1$. Generically, any epidemic process with time-varying growth rate can be written in the following form:

$$I(t+1) = I(t) \times \mathcal{R}(t) \times \eta(t). \quad (1)$$

Here, $\mathcal{R}(t)$ represents a generic time-varying parameter which indicates the number of infections that stem from each infected individual, and $\eta(t)$ represents noise in the process, which we assume to come from a log-normal distribution with parameters $\mu = 0$ and σ^2 . This choice of distribution for the noise is fundamental to the branching process literature that inspires this type of model and is a natural assumption in this setting [4].

In this work, we build upon the aforementioned model and assume individuals control the growth rate using a time-varying parameter $\rho(t) \geq 0$ which represents the proportion of existing ties that each infected individual will add or remove at time t . Mathematically, we assume $\mathcal{R}(t) = \mathcal{R}(0) \times \prod_{k=1}^t \rho(k)$, where $\mathcal{R}(0)$ is taken to be a constant value that represents the initial rate of infection. Hence, the open loop dynamics of the system considered in this work take the form

$$I(t+1) = I(t) \times \mathcal{R}(0) \times \prod_{k=1}^t \rho(k) \times \eta(t). \quad (2)$$

Although equating $\rho(t) = \mathcal{R}(t)/\mathcal{R}(t-1)$ reveals that the models in Eq. (1) and Eq. (2) are equivalent, we note that the parameterization of the model in terms of $\rho(t)$ represents a subtle but important distinction from models proposed in recent literature: rather than assume the contact rate is a direct function of a population's interventions, here we make the assumption that individuals are instead able to control the *rate* at which they increase or decrease interactions with one another. In terms of a mechanical analogy to a car, rather than assuming that individuals dictate control of position through a choice of velocity, our model assumes that individuals control their position through acceleration, i.e. by pressing on the gas or the brakes. This parameterization allows us to model the reaction of the population in a novel way, by allowing $\rho(t)$ to be a function of previous case counts, as will be shown in Eq. (4).

Connections to Existing Epidemic Models Because the time series of control parameters $\rho(t)$ is not specified in Eq. (2), the model is considered open loop, and we note that natural selections of $\rho(t)$ lead to common epidemic models in the literature. In particular, if $\rho(t) = 1$ for all t , then the model leads to *exponential growth* in case counts, which is a commonality across the initial stages of many epidemic models [10].

If $\rho(t) = \bar{\rho}$ for all t , where $\bar{\rho} < 1$, then Eq. (2) recovers the form of the Gaussian curve noted in *Farr’s law*, which is a common non-mechanistic approach to prediction of an epidemic [8].

Moreover, a detailed connection can be made to the standard SIR model. A specific time-varying choice of $\rho(t)$ can recreate the traditional *Susceptible-Infected-Recovered (SIR)* model as well as its time-varying extensions [11]. In discrete time, the SIR model consists of the following set of dynamic equations [2]:

$$\begin{aligned} S(t+1) - S(t) &= -\frac{\beta}{N} S(t)I(t) \\ I(t+1) - I(t) &= \frac{\beta}{N} S(t)I(t) - \gamma I(t) \\ R(t+1) - R(t) &= \gamma I(t). \end{aligned}$$

In the model, N represents population size, and $S(t)$, $I(t)$ and $R(t)$ represent the parts of the population that are susceptible, infected, and recovered from infection, respectively. In this simplified model, it is assumed that for all t , $S(t) + I(t) + R(t) = N$, and we use the convention that at $t = 0$ we have $I(0) = 1$, $R(0) = 0$, and $S(0) = N - 1$. The parameters β and γ modulate the dynamics of the system, where β measures the average number of contacts each individual in the population has with others, and $1/\gamma$ represents the average amount of time that an infectious individual is able to infect others. Such parameters are often allowed to be time-varying, which ultimately results in infection dynamics of the form

$$I(t+1) = I(t) \times \left[1 - \gamma(t) + \frac{\beta(t)}{N} S(t) \right]. \quad (3)$$

For any choice of time-varying $\gamma(t)$ and $\beta(t)$, these dynamics are a special case of the model Eq. (2), as we note in the following proposition, proved in the Supplementary Material.

Proposition 1. *There exists a parameterization of the open loop model in Eq. (2) such that its dynamics are equivalent to the time-varying SIR model in Eq. (3).*

The connection to the SIR model reveals that the model in Eq. (2) provides a novel way to represent how individuals react in a pandemic. Specifically, we see that the open loop model in Eq. (2) does not explicitly assume that individuals in a population are adjusting their contact rates or recovery rates. The model assumes that people are unaware of the cardinal values that govern the physics of infection dynamics, given by a particular value of $\mathcal{R}(t)$, and instead control the relative proportion of ties they add or remove from their network, which would be equivalent to $\mathcal{R}(t)/\mathcal{R}(t-1)$.

A New Model of Implicit Feedback We allow the model in Eq. (2) to incorporate implicit feedback by allowing the control parameter to take the following form:

$$\begin{aligned} \log \rho(t) &= \beta_1 \times \log I(t) + \\ &\quad \beta_2 \times (\log I(t) - \log I(t-1) - \log \mathcal{R}(0)) + \beta_3. \end{aligned} \quad (4)$$

Behaviorally, Eq. (4) implies that individuals in a population observe case counts through $\log I(t)$, and if $\beta_1 < 0$, which is the case in observed data, then larger magnitude of cases result in more control actions, for example through increased social distancing or mask adoption. Similarly, individuals react to the recent change in cases relative to the reproductive rate ($\log I(t) - \log I(t-1) - \log \mathcal{R}(0)$), and when $\beta_2 < 0$, which is again consistent with empirical observations, then individuals increase the control action if cases are rising quickly. Finally, β_3 represents a constant term which indicates an inherent level of reaction by the population. It is worth noting that if $\beta_1 = \beta_2 = \beta_3 = 0$, then $\rho(k) = 1$ in this uncontrolled case and we recover a simple model of exponential growth. Moreover, as discussed in the Supplementary Information, this assumption

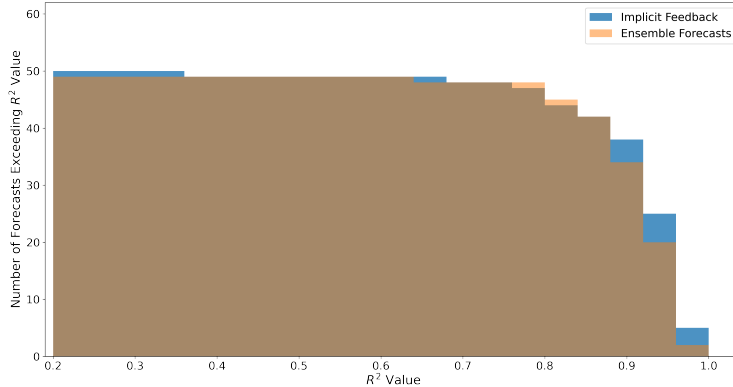


Figure 2: Comparison of R^2 values between the implicit feedback approach in Eq. (5) to ensemble forecasts [15] on each state. The plot shows the number of states for which each method has an R^2 at least that of the value on the x -axis. Calculated R^2 values can be found for each state in Table 2 of the Supplementary Information. Even though the closed model in Eq. (5) only uses 3 parameters learned in a training period, whereas the ensemble method is aggregated over multiple complex models each week, we find that the closed loop model outperforms the ensemble, particularly in the region where $R^2 > 0.85$, as is shown by the blue bars exceeding the orange. In contrast, a fixed parameter SEIR model, which also has three parameters, does not achieve positive R^2 for one week ahead forecasts on any state in the dataset.

can be viewed as creating a specific time-varying structure for the time-varying SIR model in Eq. (3). Using state feedback allows us to write the model into the single closed loop dynamical system as follows.

Let $\mathbf{X}(t) \in \mathbb{R}^3$ represent the state of a dynamical system where $X_1(t) = \log I(t-1)$, $X_2(t) = \log I(t)$, and $X_3(t)$ represents the cumulative control taken so far, i.e. $X_3(t) = \sum_{k=1}^t \log \rho(k)$. The closed loop dynamics of the system Eq. (2) under the control policy Eq. (4) are summarized by the following affine dynamical system:

$$\mathbf{X}(t+1) = \mathbf{Q}\mathbf{X}(t) + \mathbf{c} + \boldsymbol{\eta}(t). \quad (5)$$

Here,

$$\mathbf{Q} = \begin{bmatrix} 0 & 1 & 0 \\ 0 & 1 & 1 \\ -\beta_2 & \beta_1 + \beta_2 & 1 \end{bmatrix}, \text{ and } \mathbf{c} = \begin{bmatrix} 0 \\ \log \mathcal{R}(0) \\ -\beta_2 \log \mathcal{R}(0) + \beta_3 \end{bmatrix}.$$

Given the assumption that $\boldsymbol{\eta}(t)$ in Eq. (2) is log-normal, we see that $\boldsymbol{\eta}(t)$ can be modeled as unobserved Gaussian noise with mean 0 and variance σ^2 . This closed loop model is extremely simple as it is governed by only three parameters, and can be efficiently learned from data [16]. As our results indicate, the model fits the data surprisingly well, which suggests that it succinctly describes existing behavior throughout the pandemic, and the model has the critical implication that steady state infections are non-zero.

1.2 Summary of Results

With the above model, in comparing to existing data we see that there is a satisfactory fit to observed data and that the parameters of the implicit feedback correlate with observed policies. Moreover, in our analysis, we find that a major consequence of this model is that weekly cases are never eradicated; rather, for most observed learned parameters, weekly cases will stabilize at some non-zero level. This has non-trivial policy implications— in order to eradicate COVID-19 sooner rather than later, populations need to introduce another policy intervention. For example, by reacting to *total* case counts since the beginning of the pandemic rather than the case counts in the last two weeks.

Fit to Data. Our results indicate the model fits to empirical data surprisingly well, despite having only 3 learned parameters. As a means of comparison, we assess the performance of our model against the ensemble

method used by the CDC, which aggregates predictions from at least 30 state of the art forecasting models each week to provide predictions of COVID-19 case counts [15]. In Figure 2, we see that the R^2 is comparable to state of the art ensemble predictions across all 50 states, when the method is trained using 65 weeks of data. In fact, the approach outperforms the CDC point forecasts in 32 states. The implicit feedback approach also outperforms a Susceptible-Exposed-Infected-Recovered (SEIR) model, which similarly has three parameters but does not achieve a positive R^2 score on any state. An example of the one week ahead forecasts can also be seen in Figure 1, where we see similar results across data for the entire United States. We also show that other similar feedback policies do not fit as well to the data as the simple policy suggested in Eq. (4). This, combined with the comparison to observed policies noted below, gives additional credence to this choice of model.

Comparison to Observed Policies. In regressing parameters of the model against policies taken by different populations across the globe, we find significant correlations between the β_1 and β_2 parameters when compared to mobility data as well as levels of natural immunity measured by the percentage of the population which has had a confirmed positive COVID-19 test. This relationship between parameters of the model and observed policies taken by populations reinforces the validity of the model and also suggests ways in which the effect of the pandemic may be mitigated which are consistent with the prevailing public health guidance in the United States.

Impossibility of Eradication. We show that there is no selection of β_1 , β_2 , and β_3 that has been implemented by states which would result in zero weekly cases. As a result, in order to fully eliminate the COVID-19 pandemic, populations must alter their implicit strategies and deviate from the dynamical model in Eq. (5). This result is consistent with previous results on the fragility of non-pharmaceutical interventions, which suggests that even small measurement errors in the timing of a strategy can produce large increases in case counts [13]. Our results expand on this prior work by incorporating recent data, suggesting that even pharmaceutical interventions such as vaccinations are insufficient to eradicate new COVID-19 cases. Further, the results presented here are empirical in nature, and highlight properties of implemented policies.

We then conclude by presenting an example of a policy which does result in the eradication of COVID-19 cases in theory, and provide steps which suggest a time-varying schedule of vaccinations and stay at home orders which would approximate such a policy. Our results suggest that by increasing the intensity of certain policies by an order of magnitude, COVID-19 cases can be eradicated.

2 Data

The data used in order to learn the parameters of the model is taken from Johns Hopkins [7]. In preprocessing the data, we assume each time index t represents a full week to remove weekly seasonality. The dataset provides time series of case data in each state of the United States, as well as for 110 countries, which we aggregate weekly to fit the model in Eq. (5). We also use this data to compute estimates of naturalized immunity, by taking the ratio of confirmed positive tests and each region’s population to get a percentage of individuals who have had COVID-19.

In order to compare the learned parameters to observed policies, we also use data from Google [1], which compares aggregate mobility trends across individual states and countries compared to pre-pandemic levels.

3 Methods

To learn the parameters of the implicit control, we focus on identifying the parameters β_1 , β_2 , and β_3 from Eq. (4). To do so, we first infer each $\log \rho(t)$ from future time steps, as Eq. (2) yields:

$$\log \rho(t) = \log I(t+1) - \log I(t) - \sum_{k=1}^{t-1} \log \rho_k - \log \mathcal{R}(0) - \log \eta(t).$$

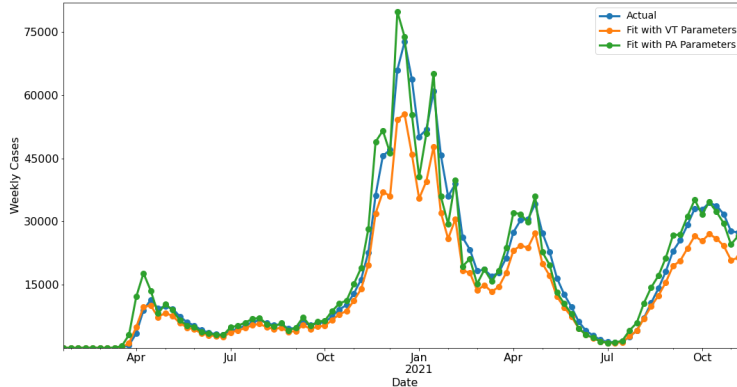


Figure 3: Applying learned parameters across different states. We find that different values of the implicit control policy correspond to dramatically different observations in case counts, suggesting that variations in the control parameters β_1 , β_2 , and β_3 are meaningful.

Hence, because $\log \eta(t)$ is mean-zero, we estimate

$$\begin{aligned} \log \rho_0 &= \log I(t+1) - \log I(t) - \log \mathcal{R}(0) \\ \log \rho(t) &= \log I(t+1) - \log I(t) - \sum_{k=1}^{t-1} \log \rho_k - \log \mathcal{R}(0) \quad (t \geq 1). \end{aligned}$$

We estimate $\mathcal{R}(0)$ to be equal to 2.5 [12], and hence we are able to infer the values of the dependent variable $\log \rho(t)$. Next, we estimate the regressors on the right hand side of Eq. (5), namely $\log I(t)$ and $\log I(t) - \log I(t-1) - \log \mathcal{R}(0)$. We then perform a least-squares regression using the inferred $\log \rho(t)$ values and the observed regressors to determine the coefficients β_1 , β_2 , and β_3 . Such an approach of using a least-squares regressions to learn the parameters of a dynamical system are not uncommon, and many theoretical results exist showing the consistency and non-asymptotic reliability of such methods [16].

We also provide statistical evidence which shows that the learned β_1 and β_2 parameters above correlate with policies taken by individuals during the pandemic. To get an estimate of policies taken during the pandemic, we process the Google mobility data, which consists of six mobility measures given as time series for each geographical region, and take the first two principal components of the data, such that for each region we get two time series. We then average this time series for each region over the time period that the policies are learned, giving two regressors for each region. Finally, we compute the correlation between the β_1 and β_2 parameter and each mobility metric. We then repeat the same procedure replacing the mobility metrics with the normalized number of cumulative cases in each region up to the end of the training period, which we use as a proxy for natural immunity.

4 Results

4.1 Fit to Observed Data

As shown in Figures 1 and 2, the use of the closed-loop model Eq. (5) fits the data well, with R^2 values comparable to the 1 week ahead CDC ensemble forecasts which aggregate predictions from over 30 state of the art prediction models [15]. It is worth noting that the CDC ensemble forecasts are used solely as a baseline to validate that the model in Eq. (5) fits well to the data. In practice, due to delays in the data collection, the observed values of $I(t)$ at time t are often underestimated, resulting in a small drop in predictive performance when only data available at each particular time is used (Supplementary Information, Figure 14). Although such data fidelity issues can be accounted for, we note that the purpose of this work is to highlight the behavioral implications of this model as opposed to its predictive value.

The learned β_1 , β_2 , and β_3 parameters are heterogenous between different geographic regions, and we find that different parameters of implicit control result in different implications for the pandemic. The 50 states

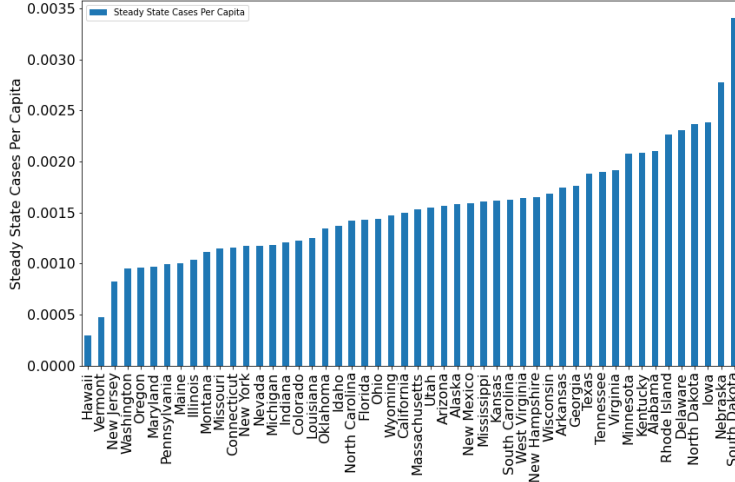


Figure 4: Computed steady state case counts per capita for each state, based on the learned parameters of the implicit control policy. These values have a 0.564 correlation with the actual mean weekly case counts per capita in each state ($p < 10^{-4}$), supporting the validity of the model Eq. (5) and suggesting particular geographic regions to focus on adjusting implicit control.

in the US provide insight into the different values of β_1 and β_2 and their importance in understanding the different forms of control that are being implicitly used by different states throughout the pandemic. The learned β_1 and β_2 parameters from each of the 50 states are shown in Figure 5, and it is clear that there is heterogeneity in the learned values.

The differences in these learned values are significant as far as their effects on prediction, as we can not simply take one state’s parameters and use this information to predict for a different state (Figure 3). While there are clusters of states with similar parameters, it is clear that the specific values of parameters is still important in terms of generating valid predictions and explaining behavior.

The learned β_1 , β_2 , and β_3 parameters can also be used in order to understand the heterogeneity in each state’s implicit control policies. When the matrix \mathbf{Q} is stable in Eq. (5), we can compute the steady state number of cases $\lim_{t \rightarrow \infty} X_2(t)$. We report the per capita results in Figure 4. This steady state value provides insight on how different states handled the pandemic in terms of the ability to efficiently bring case counts towards 0. In particular, larger steady state values seem to suggest relaxed policies in controlling pandemic.

It is worth noting that this is a compounded impact of government policies, population behavior and other circumstances (e.g. weather, industry, etc.). However, it is a definitive way to “evaluate” the compounded effect across states which may be of interest in its own right.

4.2 Relationship to Observed Policies

Our results indicate that both β_1 and β_2 correlate with observed policies taken throughout the pandemic. In comparing the learned parameters of all 50 states as well as 110 countries to observed mobility patterns, we find statistically significant correlations (Supplementary Information, Table 3). Moreover, we also see significant correlations with respect to the proportion of the population that has become immune during the training period. This suggests a relationship between learned parameters and the proportion of the population which is no longer susceptible to the disease. In fact, a similar relationship can be shown between β_1 and vaccination rates across the United States; however, the statistical evidence only suggests a correlation as the parameters are learned from the initial stages of the pandemic, so a causal relationship can not be made (Supplementary Information, Table 4).

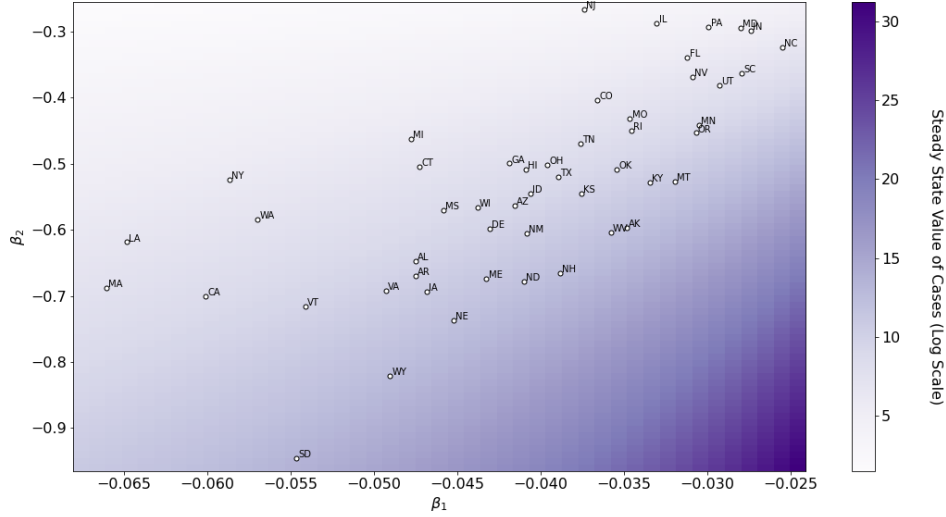


Figure 5: Coefficients of the implicit control used by the 50 US states. We find that states with low magnitude of β_2 and high magnitude of β_1 have a higher magnitude of steady state cases, highlighting a need for adjusted implicit policies in states such as South Dakota, Wyoming, and North Dakota.

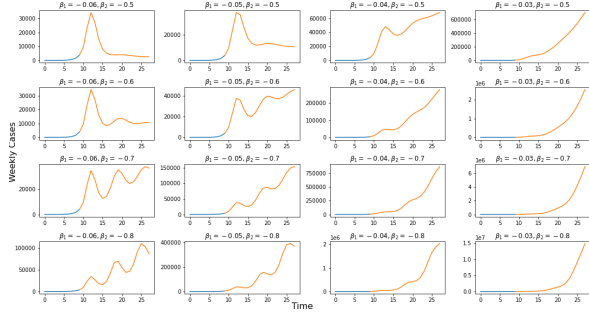
4.3 Comparisons to Other Feedback Models

While the model fits to empirical data suggest that the model is consistent with observations, and the parameters do correlate with observed policies, such results cannot definitively prove that the model assumptions are representative of reality. Here, we compare our model to other plausible hypotheses in order to understand the value and limitations of this simple approach.

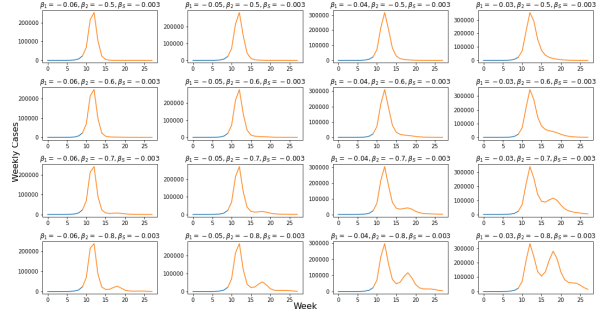
Because the results until now have provided one week ahead forecasts, and hence are dependent on most recent actual observations, it is also important to compare against a case in which these recent observations are estimated. In control theory, an observer is used for this task [3]. When implementing the system with an observer as opposed to true data on the US case counts, we find that our predictions are still very close to when the original data is used, with nearly equivalent R^2 values. This approach also provides a way to produce k -week ahead forecasts for $k > 1$, and we find that short term forecasts which predict 1 or 2 weeks ahead are comparable to the CDC ensemble, whereas longer term forecasts deteriorate rapidly (Supplementary Information, Figure 12).

We also compare this model to a simple, one-dimensional Proportional-Integral-Derivative (PID) controller, since PID control is nearly ubiquitous in control applications [6]. In this comparison, we find that the PID controller requires more data in order to effectively learn appropriate parameters, and that it does not explain the data as well as the closed-loop system in Eq. (5) (Supplementary Information, Figure 10). Hence, although PID control is omnipresent in engineering applications, it is not representative of the actual behavior observed throughout the pandemic.

Finally, we compare against several models for which different sets of regressors are used in estimating $\log \rho_t$, in order to understand the different implications of each approach (Figure 7). Our results indicate that our proposed feedback law in Eq. (4) provides the best explanation of $\log \rho_t$ across the 50 states. It is also important to note that the use of $\sum_{k=1}^t \log I(t)$ as a regressor for $\log \rho_t$ does not improve prediction performance, and that the coefficient of $\sum_{k=1}^t \log I(t)$ is never significantly away from 0 across all 50 states and countries considered. This observation indicates at least one way in which policy changes can be modified to eradicate COVID-19 cases, and will be discussed further in [Rethinking Control for Future Epidemics](#) where we discuss the policy implications of our results.



(a) Simulated policy with control consistent with population behavior (Eq. (4))



(b) Simulated policy with an added integral term (Eq. (6))

Figure 6: (a) Different choices of β_1 and β_2 for the system in Eq. (5). This simulated system begins with an initial exponential growth (blue) followed by case counts when the control policy enacted (orange). We find that as β_1 becomes closer to 0, the system becomes increasingly unstable and prone to exponential growth. As β_2 decreases away from 0 with fixed β_1 , we see that the system becomes more oscillatory and likely to become unstable as well. Moreover, across all selection of parameters, even when the system is such that \mathbf{Q} is stable, we see that the steady state number of cases is non-zero. (b) Adding an integrator term $\beta_S \sum_{k=1}^t X(k)$ to the implementation of the control input $\log \rho_t$. The simulated system again begins with an initial exponential growth (blue) followed by case counts when the control policy enacted (orange). The integral term stabilizes the system and brings weekly case counts towards an equilibrium with no weekly cases, although in practice we find that no country has a statistically significant non-zero β_S term in its control policy.

4.4 Properties of the Implicit Feedback Control

The impact of the parameters which govern the implicit feedback control is summarized in Figure 6a. Figure 6a indicates that there is a complex relationship between the values of β_1 and β_2 and the resulting case counts. Namely, increases in β_2 often result in oscillatory behavior, but still depend on the value of β_1 . These plots reflect that an equilibrium for this type of control strategy occurs at a non-zero but constant steady state of weekly cases. Stated differently, the equilibrium of this approach suggests that behavior eventually results in an instantaneous reproductive rate of 1. This reinforces that the system is sensitive to the selection of β_1 and β_2 , and our results indicate that β_1 and β_2 can be learned from data and fit the data surprisingly well (Figure 1).

4.5 Rethinking Control for Future Epidemics

Principles of control dictate that when Eq. (2) has a multiplicative factor of $\mathcal{R}(0) > 1$, the system generated when taking logarithms of Eq. (2) can be driven to 0 weekly cases using a feedback law known as a double integrator. That is, rather than the system dynamics being governed by the form of $\log \rho_t$ described in Eq. (4), a suitable control would take the form

$$\begin{aligned} \log \rho(t) = & \beta_1 \times \log I(t) + \\ & \beta_2 \times (\log I(t) - \log I(t-1) - \log \mathcal{R}(0)) + \\ & \beta_3 + \beta_S \times \sum_{k=1}^t \log I(t), \end{aligned} \quad (6)$$

where $\sum_{k=1}^t \log I(t)$ represents an integral feedback control. On synthetic data, the effect of this integrator term $\beta_S \sum_{k=1}^t \log I(t)$ is clear, as it drives weekly case counts to 0 (Figure 6b). This additional term forces the weekly reaction of the community to the pandemic to go from being a proportional derivative (PD) control in Eq. (4) to a proportional-integral-derivative (PID) control, which provides the necessary integration of error which eventually results in a steady state of 0 weekly cases.

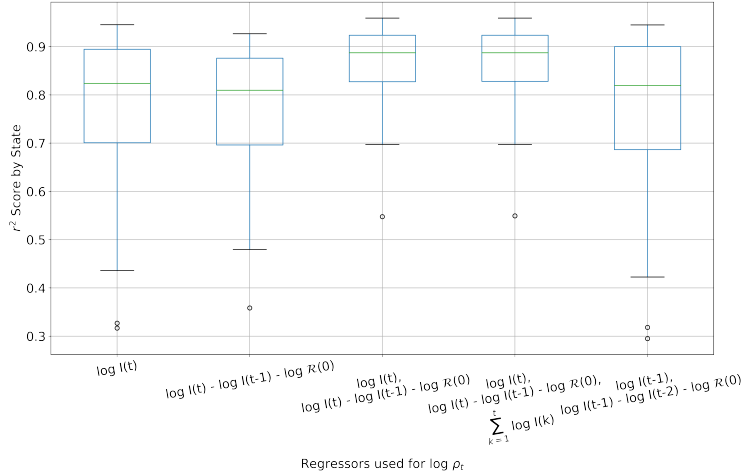


Figure 7: Boxplot of R^2 scores of the 50 US states when different regressors are used to determine $\log \rho_t$. We find that the choice of regressors in Eq. (4) provides the best fit to the data overall, suggesting that the three parameter control input fits sufficiently well across heterogenous regions. Moreover, including a regression term on $\sum_{k=1}^t \log I(k)$, as is proposed in Eq. (6) does not result in an improved fit to the data, suggesting that this particular policy which would eradicate COVID-19 cases is not being implemented by populations.

Key policy implication. Ultimately, this suggests that the *cumulative* costs of the pandemic should be emphasized, even when the current state of the pandemic has a low number of cases. When the implemented control has little memory of the past, we can not expect cases to decay towards 0. The policy implication here is *implicit*, rather than explicit, in the sense that the current policy interventions being used, such as stay at home orders, mask mandates, and vaccination development, are still suggested by this model. However, rather than implementing these policies a function of recent cases, the model suggests they should be implemented and intensified according to cumulative case counts. Moreover, because the suggestion is implicit in behavior, the model also calls for individuals in a population to adopt a slightly different latent approach that reduces contacts as a function of cumulative case counts as opposed to recent ones.

While there are many ways integral feedback can be implemented in practice, we highlight one possible policy which can be taken by adapting the existing policy in Eq. (4) using time-varying parameters. In Figure 8, we show that the integral policy suggested Figure 1 can be replicated by allowing β_1 and β_2 to be time-varying. Moreover, since we have shown that β_1 and β_2 relate linearly to observed policies such as vaccination rates and mobility above (Supplementary Information, Figure 13), this suggests that using time-varying policies can recreate an integral feedback policy. Specifically, in the United States we find that β_1 relates collinearly with vaccination rates, and that β_2 related collinearly with percentage of time individuals spend at home. Using these policy levers in a way that is consistent with Figure 8 would effectively replicate an integral feedback policy over time. Because the values of β_1 in Figure 8 are approximately ten times larger in magnitude than those learned across the 50 states, the analysis suggest that any appropriate policy would require that interventions would need to be increased by an order of magnitude in order to eradicate COVID-19 cases.

5 Discussion

We provide a dynamical model to represent the trajectory of cases in an epidemic, and show that COVID-19 cases are well explained by a control strategy which only depends on three parameters. The result is based on a robust estimation procedure, and all learned parameters are non-zero in a statistically significant sense.

While the results are strong, we note that the simplicity of the model and its implicit nature do have some drawbacks, as it is difficult to capture the known properties of the disease in this model. For example, the assumption that cases in week $t+1$ are driven by the cases in week t does not explicitly take into account

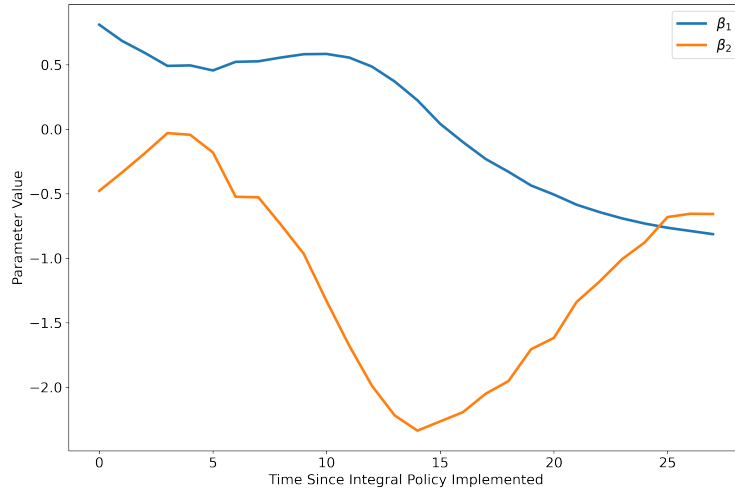


Figure 8: Example of recreating the integral feedback policy of the red line in Figure 1 using time-varying β_1 and β_2 to replicate the effect of an integral feedback term. By steadily increasing vaccination adoption according to the blue line presented above, and using stay at home orders to replicate the orange line, policy makers can effectively replicate an integral feedback policy.

possible delays in testing procedures and the amount of time it takes for an exposed individual to test positive. However, since we do find that the model is sufficient to explain variation in the data and provides a rigorous data-driven approach to estimation by making such simplifying assumptions, we believe there is value in modeling epidemic dynamics using this approach. In future work, we aim to better understand the determinants of this endogeneity, to understand why community responses to the pandemic can be easily explained by this low dimensional model. Such work would also be aimed at adapting this model for longer term predictions, as feedback is important in understanding long term trends of infectious disease [14]. As we move towards data-driven control of epidemics, our hope is to utilize this endogeneity so that policy can be designed optimally.

Ultimately, these results have important implications for the development of control strategies against infectious disease in the future. While the strategy that fits the data well does not result in an eradication of COVID-19 cases, augmenting the implicit control with a term proportional to the sum of previous case counts would eventually eradicate new cases. This suggests that policy makers should emphasize the cumulative costs of the pandemic when communicating with the public, even when current cases are low.

References

- [1] Ahmet Aktay, Shailesh Bavadekar, Gwen Cossoul, John Davis, Damien Desfontaines, Alex Fabrikant, Evgeniy Gabrilovich, Krishna Gadepalli, Bryant Gipson, Miguel Guevara, et al. Google covid-19 community mobility reports: anonymization process description (version 1.1). 2020.
- [2] Linda JS Allen. Some discrete-time si, sir, and sis epidemic models. *Mathematical biosciences*, 124(1):83–105, 1994.
- [3] Karl Johan Åström and Richard M Murray. *Feedback systems*. Princeton university press, 2010.
- [4] Krishna B Athreya and Peter E Ney. *Branching Processes*. Springer, 1972.
- [5] Victor Chernozhukov, Hiroyuki Kasahara, and Paul Schrimpf. Causal impact of masks, policies, behavior on early covid-19 pandemic in the us. *Journal of Econometrics*, 220(1):23–62, 2021.
- [6] Lane Desborough and Randy Miller. Increasing customer value of industrial control performance monitoring-honeywell’s experience. In *AICHE symposium series*, number 326, pages 169–189. New York; American Institute of Chemical Engineers; 1998, 2002.

- [7] Ensheng Dong, Hongru Du, and Lauren Gardner. An interactive web-based dashboard to track covid-19 in real time. *The Lancet infectious diseases*, 20(5):533–534, 2020.
- [8] William Farr. Progress of epidemics. pages 16–20, 1840.
- [9] Nicholas C Grassly and Christophe Fraser. Mathematical models of infectious disease transmission. *Nature Reviews Microbiology*, 6(6):477–487, 2008.
- [10] Herbert W Hethcote. The mathematics of infectious diseases. *SIAM review*, 42(4):599–653, 2000.
- [11] William Ogilvy Kermack and Anderson G McKendrick. A contribution to the mathematical theory of epidemics. *Proceedings of the royal society of london. Series A, Containing papers of a mathematical and physical character*, 115(772):700–721, 1927.
- [12] Kevin Linka, Mathias Peirlinck, and Ellen Kuhl. The reproduction number of covid-19 and its correlation with public health interventions. *Computational Mechanics*, 66(4):1035–1050, 2020.
- [13] Dylan H Morris, Fernando W Rossine, Joshua B Plotkin, and Simon A Levin. Optimal, near-optimal, and robust epidemic control. *Communications Physics*, 4(1):1–8, 2021.
- [14] Hazhir Rahmandad and Tse Yang Lim. Risk-driven responses to covid-19 eliminate the tradeoff between lives and livelihoods. *Available at SSRN 3747254*, 2020.
- [15] Evan L Ray, Nutchana Wattanachit, Jarad Niemi, Abdul Hannan Kanji, Katie House, Estee Y Cramer, Johannes Bracher, Andrew Zheng, Teresa K Yamana, Xinyue Xiong, et al. Ensemble forecasts of coronavirus disease 2019 (covid-19) in the us. Cold Spring Harbor Laboratory Press, 2020.
- [16] Tuhin Sarkar and Alexander Rakhlin. Near optimal finite time identification of arbitrary linear dynamical systems. In *International Conference on Machine Learning*, pages 5610–5618. PMLR, 2019.
- [17] Greg Stewart, Klaskevan Heusden, and Guy A Dumont. How control theory can help us control covid-19. *IEEE Spectrum*, 57(6):22–29, 2020.
- [18] Klaske Van Heusden, Greg Stewart, Sarah P Otto, and Guy A Dumont. Pandemic policy design via feedback: A modelling study. *Available at SSRN 3928502*, 2021.

Supplementary Information

A Proof of Proposition 1

Proof. First, note that for the two models to be equivalent, we must take the noise parameter in Eq. (2) to be a constant, i.e. $\sigma^2 = 0$. We then construct the parameterization as follows: For arbitrary but particular time series $\beta(t)$ and $\gamma(t)$, first define

$$\mathcal{R}^{SIR}(t) = 1 - \gamma(t) + \frac{\beta(t)}{N}S(t).$$

Then, for

$$\mathcal{R}(0) = \mathcal{R}^{SIR}(0), \quad \text{and} \quad \forall t \geq 1, \quad \rho(t) = \frac{\mathcal{R}^{SIR}(t)}{\mathcal{R}^{SIR}(t-1)}, \quad ,$$

the model in Eq. (2) is equivalent to the time-varying SIR model in Eq. (3). \square

B Connection Between the Closed Loop Model and Time-Varying SIR Model

We note there is a connection between the SIR model in Eq. (3) and the closed loop model in Eq. (5) in the sense that Eq. (4) implies a particular structure for the time-varying parameters in Eq. (3). Specifically, we see that from Eq. (4),

$$\rho(t) = I(t)^{\beta_1} \left(\frac{I(t)}{I(t-1)} \right)^{\beta_2} \mathcal{R}(0)^{-\beta_2} e^{\beta_3}. \quad (7)$$

Furthermore, from the above proof of Proposition 1, we see that the open loop model and the time-varying SIR model are equivalent so long as

$$\rho(t) = \frac{N - N\gamma(t) + \beta(t)S(t)}{N - N\gamma(t-1) + \beta(t-1)S(t-1)}. \quad (8)$$

Equating these two representations of $\rho(t)$, we find that if $\gamma(t)$ and $\beta(t)$ obey

$$\left(\frac{\gamma(t)}{\gamma(t-1)} \right) \left(\frac{\frac{N + \beta(t)S(t)}{\gamma(t)} - N}{\frac{N + \beta(t-1)S(t-1)}{\gamma(t-1)} - N} \right) = I(t)^{\beta_1} \left(\frac{I(t)}{I(t-1)} \right)^{\beta_2} \mathcal{R}(0)^{-\beta_2} e^{\beta_3}, \quad (9)$$

which can be done by equating terms of the product with one another, then the two models can be equivalent. For example, if for all $t \geq 1$,

$$\frac{\gamma(t)}{\gamma(t-1)} = I(t)^{\beta_1} e^{\beta_3}, \quad \text{and} \quad \frac{\frac{N - \beta(t)S(t)}{\gamma(t)} - N}{\frac{N - \beta(t-1)S(t-1)}{\gamma(t-1)} - N} = \left(\frac{I(t)}{I(t-1)} \right)^{\beta_2} \mathcal{R}(0)^{-\beta_2}, \quad (10)$$

then we see a specific choice of $\beta(t)$ and $\gamma(t)$ can be imposed by the closed loop model in Eq. (5). Specifically, this particular choice would result in

$$\gamma(t) = \left(\prod_{k=1}^{t-1} I(k) \right)^{\beta_1} e^{t\beta_3} \gamma(0),$$

and

$$\beta(t) = \left(N - \gamma(t) \left(\left(\frac{I(t)}{I(t-1)} \right)^{\beta_2} \mathcal{R}(0)^{-\beta_2} \left(\frac{N - \beta(t-1)S(t-1)}{\gamma(t-1)} - N \right) + N \right) \right) / S(t).$$

That is, one possible interpretation of the implicit feedback policy is that the magnitude of $\gamma(t)$ increases as the cumulative product of cases increases, and that $\beta(t)$ is inversely proportional to the remaining susceptible population and is a complex function of recovery rates $\gamma(t)$ and the rate of change of cases $I(t)/I(t-1)$.

C Additional Figures

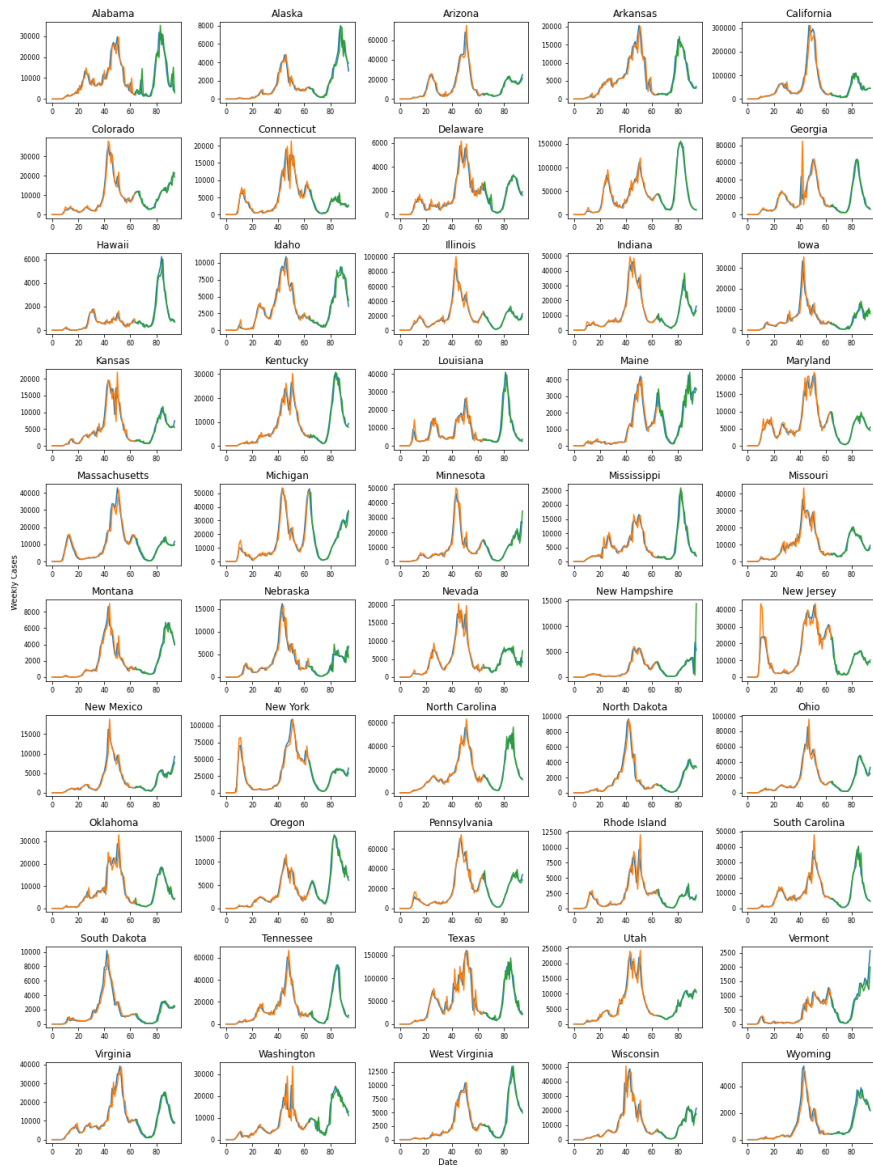
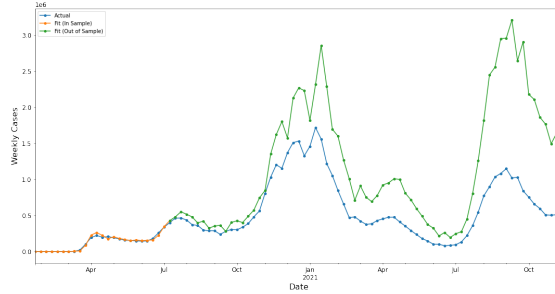
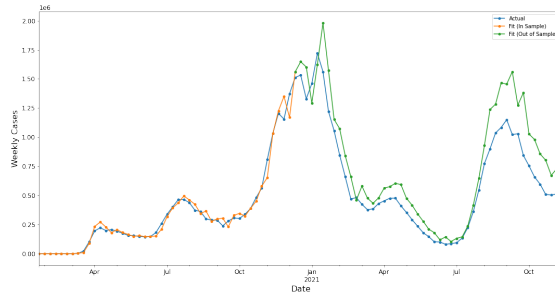


Figure 9: Case counts of US states as modeled by the dynamical system. One week ahead predictions using this method are shown in orange (in sample) and green (out of sample), and the true data is shown in blue. We find that using data from roughly the first year of the pandemic results in surprisingly accurate performance on later data.

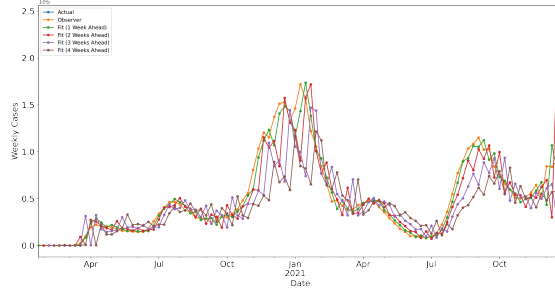


(a) PID controller learned with data from the first wave of the COVID-19 pandemic in the United States.

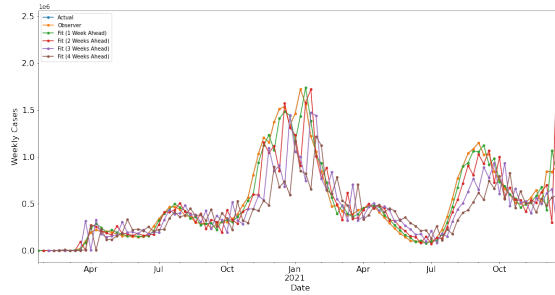


(b) PID controller learned with data from the first two waves of the COVID-19 pandemic in the United States.

Figure 10: Implementation of a PID controller learned using the single state $X(t) = \log I(t)$ (i.e., $X_2(t)$ in Eq. (5)). The PID controller has the form $u(t) = k_P X(t) + k_I \sum_{\tau=1}^t X(\tau) + k_D (X(t) - X(t-1))$, and we assume the system has the form $X(t+1) = X(t) + u(t)$. Learning for the first two waves results in an out of sample R^2 value of 0.085, and from the first three waves results in $R^2 = 0.81$, compared to an R^2 of 0.905 using the model in Eq. (5) trained on the first two waves of data, implying that the PID method requires more data to provide a worse explanation out of sample. This suggests the model in Eq. (5) provides a better fit to the data.



(a) Predictions using statistical estimates.



(b) Predictions using estimates from an observer system.

k	1	2	3	4
Statistical Estimates	0.949	0.607	0.267	-1.562
Observer System	0.949	0.607	0.267	-1.562
CDC Baseline	0.942	0.861	0.765	0.648

Table 1: r^2 Comparison of k -week ahead forecasts

Figure 12: k -week ahead forecasts using the system in Eq. (5) using statistical estimates (a) or an observer model (b) which uses an estimate of $X_1(t)$. For statistical estimates, future values of $X_1(t)$ are estimated through feeding back estimates into Eq. (5), and for the observer system a parallel system is used. We find that using the observer system results in the same performance compared to the statistical method, and that the closed loop method works best in the short term for 1 to 2 week ahead predictions.

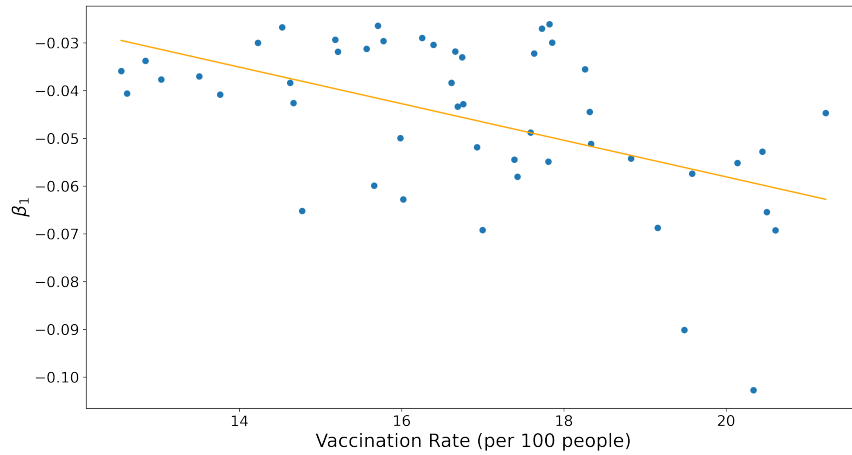


Figure 13: Comparison of learned β_1 parameters in each state to observed vaccination rates from <https://github.com/owid/covid-19-data>, where each point represents a state and the orange line is the line of best fit. We see that higher vaccination rates correspond to larger magnitudes of the β_1 parameter.

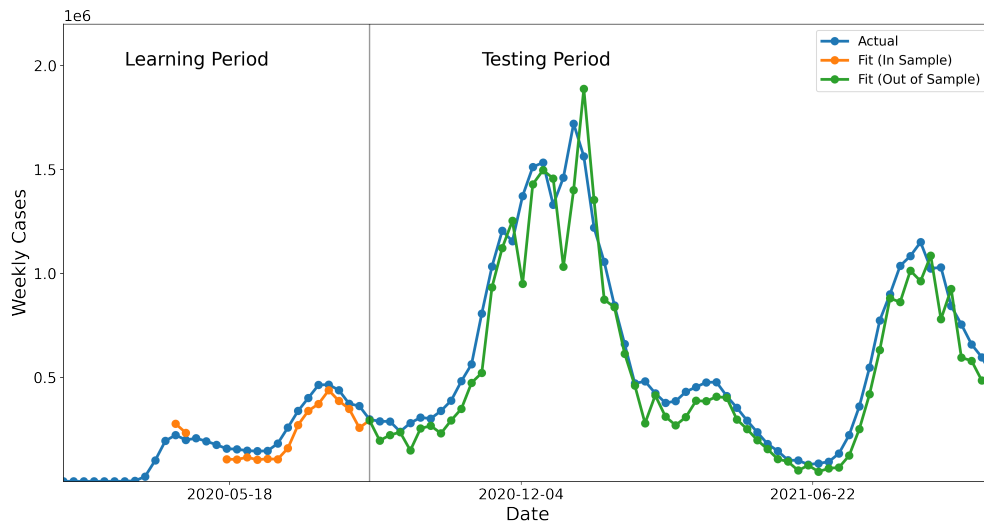


Figure 14: Forecasts of United States COVID-19 Cases using data available at each date. Because case data is adjusted after the fact, we find that using data available at each date results in a small deterioration in prediction performance, with an out of sample R^2 score of 0.901 as opposed to 0.948 using data as of March 2022.

State	R^2 of Implicit Feedback Predictions	R^2 of CDC Forecasts	R^2 of SEIR Model
Alabama	0.761268	0.870218	-7.466713
Alaska	0.895081	0.860655	-6.097458
Arizona	0.948373	0.912740	-16.846574
Arkansas	0.919352	0.904562	-5.102133
California	0.846362	0.815874	-38.857268
Colorado	0.912670	0.928491	-17.163285
Connecticut	0.787693	0.770680	-13.130171
Delaware	0.901341	0.960540	-23.524277
Florida	0.984187	0.934497	-16.086748
Georgia	0.967953	0.951781	-29.483336
Hawaii	0.910708	0.919715	-3.725094
Idaho	0.936136	0.919588	-86.226929
Illinois	0.923297	0.902908	-25.749134
Indiana	0.902190	0.925885	-61.444810
Iowa	0.813681	0.777314	-8.914433
Kansas	0.930767	0.851023	-8.554606
Kentucky	0.961193	0.927413	-4.442309
Louisiana	0.895427	0.894736	-25.563110
Maine	0.854193	0.871618	-13.050083
Maryland	0.941903	0.949353	-29.439844
Massachusetts	0.920278	0.905620	-12.569417
Michigan	0.937189	0.953322	-20.089249
Minnesota	0.876778	0.852998	-8.951495
Mississippi	0.931766	0.887371	-5.910868
Missouri	0.952072	0.903154	-12.156490
Montana	0.956009	0.956591	-3.621835
Nebraska	0.648975	0.606238	-16.876655
Nevada	0.786819	0.794385	-32.207349
New Hampshire	0.337766	0.012839	-32.442966
New Jersey	0.913044	0.947180	-7.806754
New Mexico	0.918922	0.858679	-12.438151
New York	0.948178	0.925340	-8.925778
North Carolina	0.892444	0.908425	-7.784810
North Dakota	0.969735	0.964937	-3.343721
Ohio	0.965163	0.950134	-19.912066
Oklahoma	0.957803	0.922573	-7.961322
Oregon	0.949682	0.935502	-2.391805
Pennsylvania	0.937376	0.950664	-20.954253
Rhode Island	0.756697	0.821439	-17.282322
South Carolina	0.905781	0.915286	-9.553737
South Dakota	0.929809	0.936414	-13.868844
Tennessee	0.935708	0.920788	-41.321343
Texas	0.884807	0.915912	-10.169516
Utah	0.945423	0.865068	-16.726585
Vermont	0.832917	0.819457	-45.831707
Virginia	0.956532	0.954946	-16.765430
Washington	0.847929	0.893503	-5.760364
West Virginia	0.957164	0.947691	-2.813714
Wisconsin	0.897933	0.870112	-12.464855
Wyoming	0.924037	0.919302	-9.180029
Mean	0.891370	0.877309	

Table 2: r^2 metric of 1 week ahead forecasts using the implicit feedback approach summarized in Eq. (5) compared to the r^2 scores of 1 week ahead forecasts from a state of the art ensemble model [15] and a simple SEIR model [10].

Dependent Variable	Independent Variable	Coefficient Value	p -value	Null Hypothesis Rejected
β_2	Mobility Component 2	0.006	< 0.001	✓
β_2	Natural Immunity (%)	16.852	< 0.001	✓
β_2	Mobility Component 1	0.002	< 0.001	✓
β_1	Mobility Component 2	0.001	0.001	✓
β_1	Natural Immunity (%)	5.233	0.001	✓
β_1	Mobility Component 1	0.000	0.443	

Table 3: Hypothesis tests comparing different policies to learned β_1 and β_2 values across both US states and countries around the globe. Across heterogeneous regions, we find that β_1 and β_2 tend to correlate significantly with observed measures such as mobility and the level of natural immunity.

Dependent Variable	Independent Variable	Coefficient Value	p -value	Null Hypothesis Rejected
β_1	Vaccination Rate (%)	-0.004	< 0.001	✓
β_1	Mobility Component 2	-0.000	0.004	✓
β_1	Mean Distance Traveled From Home	-0.028	0.007	✓
β_2	Median Percentage Time Home	0.016	0.018	✓
β_2	Mean Distance Traveled From Home	-0.210	0.044	
β_2	Mobility Component 1	-0.001	0.056	
β_1	Median Time Spent Away From Home	0.000	0.064	
β_2	Vaccination Rate (%)	-0.019	0.073	
β_1	Mask Mandate	-0.017	0.079	
β_2	Natural Immunity (%)	7.116	0.128	
β_2	Mobility Component 2	0.002	0.184	
β_1	Natural Immunity (%)	0.608	0.210	
β_2	Mask Mandate	-0.057	0.550	
β_2	Median Time Spent Away From Home	-0.001	0.582	
β_1	Median Percentage Time Home	-0.000	0.853	
β_1	Mobility Component 1	-0.000	0.962	

Table 4: Hypothesis tests comparing different policies to learned β_1 and β_2 values in the United States only. We find that β_1 correlates with vaccination rates in each state as well as mobility, and that β_2 correlates with mobility metrics. Here, vaccination data is taken from <https://github.com/owid/covid-19-data> and mobility auxiliary mobility data is taken from SafeGraph (“Median Time Spent Away From Home,” “Mean Distance Traveled From Home,” , “Median Percentage Time Home”) and Google (Mobility Components 1 and 2, which are principal components of the 6 mobility metrics provided by Google).